Photopolymerization Studies Using Visible Light Photoinitiators[1]

O. Valdes-Aguilera,* C. P. Pathak, J. Shi, D. Watson, and D. C. Neckers*

Center for Photochemical Sciences, Bowling Green State University, Bowling Green, Ohio 43403

Received June 4, 1991; Revised Manuscript Received August 28, 1991

ABSTRACT: We have synthesized six esters of decarboxylated Rose Bengal and employed them as electron-donor photoinitiators at 514 nm. Photoreduction of the dyes by triphenyl *n*-butyl borate ion in ethyl acetate yields decarboxylated Rose Bengal (RB) as well as products that do not adsorb in the visible region. The yield of RB is approximately 8% of total dye consumption and is produced by cleavage of the radical anion formed in the initial electron-transfer step. We have studied the photopolymerization of polyol acrylates initiated by the RB esters plus electron donor under steady-state irradiation with the Ar^+ laser, $\lambda = 514$ nm. Photopolymerization results in thin films as well as in thick samples indicate the order with respect to light intensity is 0.5 at both low and relatively high conversions (40%). The ratio $k_p/k_t^{0.5}$ depends on the identity of the RB ester employed as photoinitiator. On the basis of our results, we conclude that the initiating radical is derived from the electron donor whereas the radical released by cleavage of the semireduced dye acts as the predominant terminator of polymer chains.

Introduction

In commercial practice, most compounds which absorb light and produce a chain-initiating event, photoinitiators, operate below 400 nm. After absorption they yield free radicals by either a Norrish type 1 split (benzoin ethers or ketone acetals) or electron transfer (benzophenone tertiary amine). In practice, most monomers used in photoinitiated polymerization are acrylates or modified acrylates whose structure lends to rapid cross-linking. Since oxygen terminates free-radical chains and free-radical polymerizations are quenched by oxygen, one adds an accelerator, often a tertiary amine, the purpose of which is to, apparently, ameliorate this effect.[2]

In recent years photoinitiators which operate in the visible region of the spectrum have also been developed. These initiators absorb light which is blue, green, or red and, with speed which is near photographic, cause the same photopolymerization events described above to take place—namely conversion of a highly functionalized liquid acrylate monomer to a solid polyacrylate. Some of these photoinitiators have been widely discussed in contemporary popular science literature for they are the backbone of non-silver, near-photographic speed, photopolymerization.[3] In one such process, Mead's Cycolor process,[4] the initiators are cyanine dye borate ion salts—so-called (+, −) ion-pair initiators—which utilize single electron transfer to the excited state of the light-absorbing dye from the gegen or partner ion as the crucial first step in initiating the radical chain. Thus, the cyanine dye, in its excited state, accepts an electron from the partner borate, and subsequent boranyl radical chemistry initiates polymerization. Other initiators active in the visible have been invented by us.[5] These are xanthene dye onium salt (−,+) ion-pair photoinitiators which function by oxidation of the excited state of the dye, rather than reduction.

Cycolor was the first commercial product of which we are aware to use visible light systems for the photoinitiation of polymerization. The wavelength of absorption of the cyanine borate initiator is tuneable by means of the number of conjugated alkene units, the number *n* in the cyanine dye. In the intimate ion pair, the cyanine dye in its excited singlet state rapidly oxidizes the borate anion by single electron transfer and the boranyl radical cation, decomposes forming an aryl radical which initiates the chain as well as triarylboron (Figure 1).

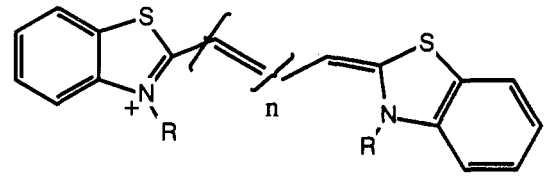

Ar_3BR^-

Figure 1. Structure of a thiocyanine borate.

Cyanine borates make prime candidates for use with the argon ion laser (488, 514 nm) and the helium/neon laser (632 nm). However, these systems are much more highly absorbing than the typical UV photoinitiator; thus, they preclude the formation of polymer in anything but infinitely thin films when used as they are used in concentrations sufficient to provide near-photographic speed. In order for laser-initiated photopolymerization to occur at any depth below the surface plane *x*,*y* of a highly functionalized cross-linkable monomer solution containing the initiator therefore, the absorbance of the initiator must disappear at a rate similar to the act of causing photopolymerization. In other words, concomitant bleaching of the initiator is required during the initiation in order for anything more than a surface cure to take place.

We, and others, have specifically studied Eosin as a photoinitiator for the purpose of initiating polymerization in depth.[6] Eosin's spectral properties in polar solvents such as methanol (absorption, $\lambda_{max} = 528$ nm, $\epsilon_{max} = 1.1 \times 10^5$ M^{-1} cm^{-1}; emission, $\lambda_{fl} = 547$ nm, $\phi_f = 0.59$) are such that it is also almost perfectly suited as a potential initiating system for the argon ion laser ($\lambda = 514$ nm). With electron donors such as triethylamine or triethanolamine, it polymerizes acrylates when irradiated and it bleaches by means of known chemistry.[7,8] The mechanism involves reductive electron transfer to the dye from the amine followed by proton loss from the triethanolamine radical cation ($TEOA^{\bullet+}$). The α-amino radical ($TEOA^{\bullet}$) formed is the initiating radical.

Eosin/triethanolamine initiating systems also have certain limitations in three-dimensional imaging applications.[9] Therefore, as part of the program Photopolymerization in Three Dimensions, we sought better initiators by means of which to accurately control polymerization of a liquid monomer in all three dimensions *x*, *y*, and *z*

0024-9297/92/2225-0541$03.00/0

relative to an initiating laser beam of some dimension striking an x,y monomer surface in the z direction (Figure 2). Our goal was to produce an initiator radical by a photochemical process which would allow for long chains, and hence the formation of a mechanically more stable polymer.

In the search for such initiators for three-dimensional imaging applications, we have developed a new group of visible light photoinitiators and we describe them herein.

Initiator System

The reader may, perhaps, recognize I as being a derivative prepared from Rose Bengal which is first decarboxylated and then acetylated. We refer to I as RBAX. On a more general basis RBAX is a xanthone, analogous

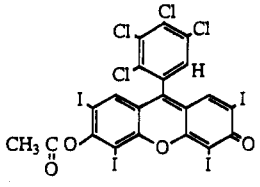

I, RBAX

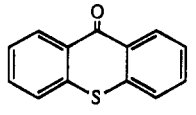

thioxanthone

to the thioxanthones which are common commercial UV photoinitiators. The latter are used with typical tertiary amine accelerators and therefore can be described, as can benzophenone/Michler's ketone, as electron-transfer UV photoinitiators. In other words, the first step in the mechanism of their initiating polymerization is electron transfer from a donor—a tertiary amine—to one or another thioxanthone excited state. On the basis of the known photoreduction chemistry of Rose Bengal,[10] one would anticipate that electron transfer would reduce the xanthene skeleton of RBAX and that the radical anion thence formed might decay by the elimination of an acetyl radical. Acetyl is totally analogous to benzoyl, which is the radical which initiates chains in the case of most Norrish type 1 UV photoinitiators, i.e., benzoin ethers or acetophenone acetals. The putative scheme is shown:

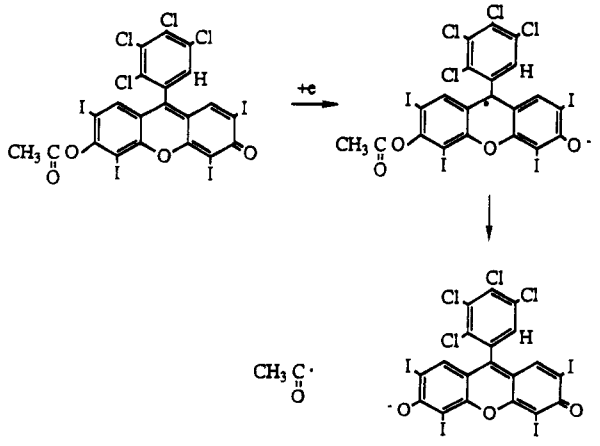

Among the experimental limitations on the electron donor is that it must not catalyze the hydrolysis of the RBAX. It cannot, therefore, be a highly basic amine. We have chosen, therefore, to study the photoreduction of RBAX in the presence of a nonhydrolytic donor, a soluble triphenyl n-butyl borate.

Experimental Section

Synthesis of RBAX. Rose Bengal was decarboxylated following suggested literature procedures by heating in DMF.[11] The decarboxylated product (hereafter RB) was purified first by washing with copious quantities of water and then with hexane.

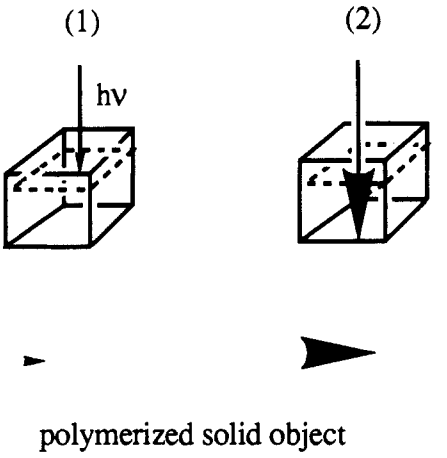

Figure 2. Schematic representation of photopolymerization at depth.

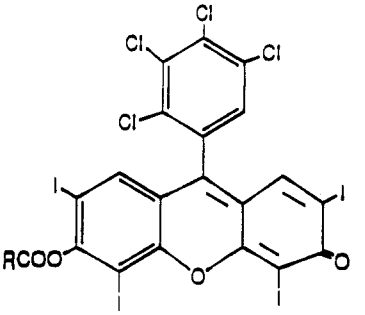

Derivative	R
1	Me
2	C_6H_5
3	$C_6H_2(OMe)_3$ [3,4,5 Methoxy]
4	$OCH_2C_6H_5$
5	OEt
6	$OCH(Me)_2$

Figure 3. Structure of visible light photoinitiators.

The red pasty solid so obtained was dried for 48 h under vacuum. NMR (DMSO-d_6) δ 7.65 (s, 2 H), 7.88 (s, 1 H).

RB (3.20 g, 0.32 mmol) was dissolved in 20 mL of acetyl chloride and the solution refluxed with stirring under argon for 36 h after which time the solution was found devoid of starting dye by TLC (silica gel/eluting solvent diethylene glycol dimethyl ether). The solution was evaporated and the brown solid further purified by column chromatography. The final product is identified as RBAX. NMR (DMSO-d_6) δ 7.62 (s, 1 H), 7.52 (s, 1 H), 7.40 (s, 1 H), 2.50 (s, 3 H).

To study the effect of substituents on the photochemistry and photopolymerization rate, we prepared a number of derivatives related to RBAX. The general structure of these compounds is shown in Figure 3, where RBAX corresponds to R = Me.

The derivatives in Figure 3 were prepared by adding the corresponding acid chloride (0.75 mmol) to 0.5 mmol of decarboxylated Rose Bengal suspended in 40 mL of chloroform. The suspension became clear as 1.0 mmol of pyridine is added dropwise at 0 °C. After being stirred at room temperature for 30–60 min, the solution is concentrated to about 15 mL. The products were purified by silica gel chromatography using methylene chloride as eluent to yield the pure compounds in 80–85% yield.

Photoreduction Chemistry. Photoreduction of RBAX by triphenyl n-butyl borate ion (Bo^-) was studied spectrophotometrically in ethyl acetate. Experiments were carried out either in aerated solutions or after purging with argon for approximately 10 min. Cetylpyridinium triphenyl n-butyl borate was a gift from Mead Imaging, Miamisburg, OH. Samples were irradiated at 514 nm with a Spectra Physics 2016 argon ion laser. The beam was expanded to form a circle of 0.9-cm diameter. The power delivered was measured with a calibrated Sciencetech 365 power meter. All absorption spectra were determined on a

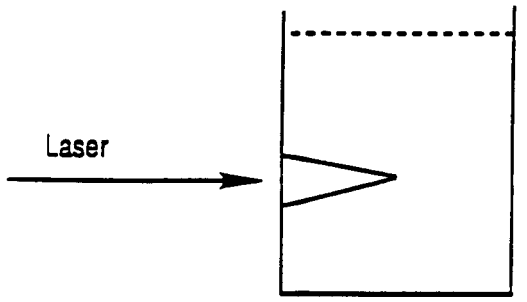

Figure 4. Schematic representation of spike formation upon laser irradiation.

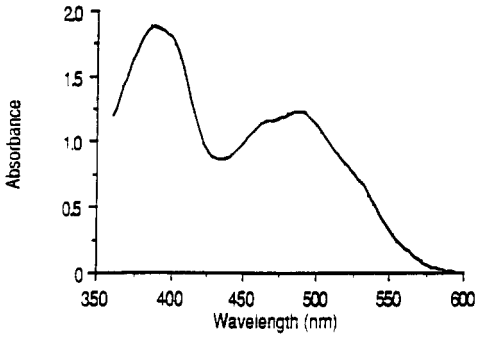

Figure 5. Visible absorption spectrum of RBAX (1.19×10^{-4} M) in ethyl acetate.

Hewlett-Packard 8452A diode array spectrophotometer. Ethyl acetate, Aldrich HPLC grade, was used as received.

Triplet lifetimes were measured at room temperature by laser flash photolysis. A frequency doubled YAG:Nd laser (532 nm, 10-ns pulse) was used for excitation. Measurements were performed both in aerated solutions and in samples subjected to continuous bubbling of argon.

Trimethylolpropane triacrylate (TMPTA) was a gift from Mead Imaging. Hexanediol diacrylate (HDDA) and dipentaerythritol hydroxypentaacrylate (DPHPA) were obtained from Sartomer and used without further purification. 1-Vinyl-2-pyrrolidinone (VP) and *N*-phenylglycine (NPG) were purchased from Aldrich and used as received.

Photopolymerization in thin films was carried out at 514 nm, the rate of heat evolution being measured by thin foil photocalorimetry.[12] The monomer formulation consisted of 85% TMPTA and 15% HDDA, giving a concentration of double bonds of 10.8 M. Irradiation was carried out with the argon ion laser, the beam being expanded to a circle of 1.1-cm diameter. The sample containing RBAX, borate, and the monomer formulation was placed between glass cover slides using lens tissue (E. H. Sargent & Co.) as a spacer. The thickness of the film produced was 25 μm, estimated by measuring the visible absorption spectrum of di-*n*-butyltetramethylindocarbocyanine borate. The absorption maximum of the cyanine is at 556 nm, and the molar absorptivity in acrylate monomers[13] is 1.8×10^5 M^{-1} cm^{-1}. The conversion of double bonds was measured by IR spectroscopy. Irradiation was carried out for a sample placed between sodium chloride plates, and the decrease of the absorption at 810 cm^{-1} was determined using a Nicolet 20DX FTIR spectrometer.

Photopolymerization rates in thick samples were determined gravimetrically. The monomer formulation was 90% DPHPA/10% VP, and the electron donor was *N*-phenylglycine. Irradiation was carried out in glass cuvettes with the argon ion laser, the beam diameter being 1.4 mm. Bleaching of the photoinitiator during the irradiation allows the photopolymerization to occur at depth and to form a solid spike (Figure 4), the dimensions of which depend on the irradiation time and the laser power. The spike is washed with acetone and dried until a constant weight is obtained.

Results and Discussion

Figure 5 presents the absorption spectrum of RBAX (1.19×10^{-4} M) in ethyl acetate. The molar absorptivities at 384 and 486 nm are 1.63×10^4 and 1.03×10^4 M^{-1} cm^{-1}, respectively. The spectral shape as well as the molar absorptivities are similar to those reported for nonpolar derivatives of Rose Bengal.[14] Irradiation of the solution for 20 min at 514 nm ($I_0 = 1.26 \times 10^{-4}$ einstein/L s) produces no change in the absorption spectrum.

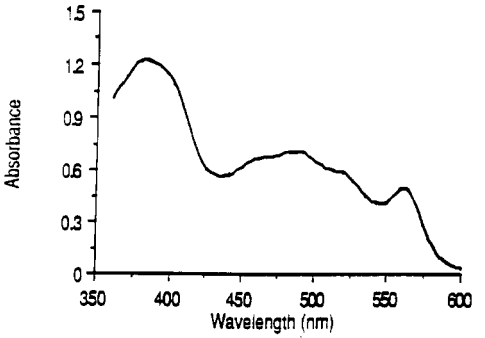

Figure 6. Visible absorption spectrum observed after irradiation of RBAX (1.19×10^{-4} M) in ethyl acetate in the presence of triphenyl *n*-butyl borate ion 1.89×10^{-3} M. Irradiation time is 2 s, and the incident light intensity is 0.17 einstein/L s.

Irradiation of RBAX (1.19×10^{-4} M) in the presence of triphenyl *n*-butyl borate ion (1.89×10^{-3} M) results in the bleaching of RBAX and the appearance of an absorption peak at 560 nm (Figure 6). This wavelength corresponds to λ_{max} for decarboxylated Rose Bengal. In addition, fluorescence measurements show that the excitation spectrum is identical with the absorption spectrum of RB. The bleaching products have not been isolated. Based on the known products for bleaching of Rose Bengal under reductive conditions[7] and the fact that oxidation of the triphenyl *n*-butyl borate ion generates the butyl radical,[13] we expect the formation of the coupling product between RBAX and the butyl group. Therefore, the reaction can be represented as

$$\text{RBAX} + \text{Bo}^- \xrightarrow{h\nu} \text{bleaching product} + \text{RB} + \text{Ph}_3\text{B}$$

The quantum yields of RBAX bleaching and of RB generation were determined by measuring the decrease of the absorption at 486 nm and the increase in absorption at 560 nm as a function of light intensity and Bo^- concentration. A summary of our results follows.

(a) The rates of RBAX bleaching, $-d[RBAX]/dt$, and generation of decarboxylated Rose Bengal, $d[RB]/dt$, vary linearly with absorbed light intensity in the range between 1.0×10^{-5} and 1.2×10^{-4} einsteins/L s.

(b) $\phi(RB)/\phi(-RBAX)$ is $(8.6 \pm 1.2) \times 10^{-2}$, independent of light intensity, Bo^- concentration (1.0–24 mM), and the presence of air.

(c) In argon-saturated solution and $[Bo^-] = 1.89 \times 10^{-3}$ M, the quantum yield for bleaching of RBAX is 0.31.

The effect of Bo^- concentration on the quantum yield for photoreduction of RBAX in aerated solutions is presented in Figure 7. The solid line is calculated by the equation describing saturation kinetics with a quantum yield of 0.39 ± 0.03 at infinite Bo^- concentration. In view of the low Bo^- concentrations required to observe the photoreduction, we conclude that the reactive excited species is the triplet state of RBAX. Measurements of the lifetime of RBAX triplet by laser flash photolysis[15] yield values of 3.64 μs in argon-saturated solution and 288 ns in the presence of air. These lifetimes are independent of the energy of the laser pulse (0.2–3 mJ/pulse) and of the concentration of RBAX ground state in the range between 1.74×10^{-5} and 2.23×10^{-4} M.

A mechanism consistent with these observations is presented in Scheme I, where *n*-Bu$^\bullet$ and Ac$^\bullet$ represent *n*-butyl and acetyl radicals, respectively.

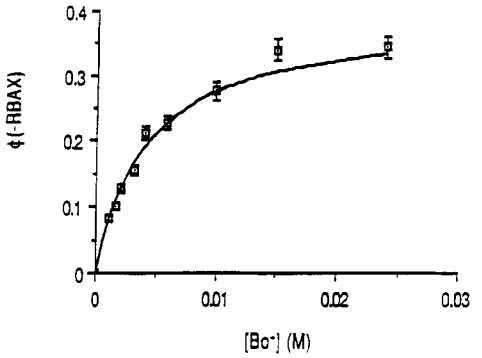

Figure 7. Effect of the concentration of triphenyl *n*-butyl borate ion on the quantum yield of RBAX photoreduction. The solid line is calculated by the equation $\phi(-\text{RBAX}) = A[\text{Bo}^-]/(B + [\text{Bo}^-])$, with $A = 0.39 \pm 0.03$ and $B = (4.16 \pm 0.21) \times 10^{-3}$ M.

Scheme I
Mechanism for Photoreduction of RBAX by Triphenyl *n*-Butyl Borate Ion in Ethyl Acetate

$$\text{RBAX} \xrightarrow{h\nu} \text{RBAX (T)}\ (I_a\phi_T)$$

$$\text{RBAX (T)} \rightarrow \text{RBAX}\ (k_1)$$

$$\text{RBAX (T)} + \text{O}_2 \rightarrow \text{RBAX} + \text{O}_2\ (k_2)$$

$$\text{RBAX (T)} + \text{Bo}^- \rightarrow \text{RBAX} + \text{Bo}^-\ (k_3)$$

$$\text{RBAX (T)} + \text{Bo}^- \rightarrow \{\text{RBAX}^{\bullet-}\ n\text{-Bu}^\bullet\} + \text{Ph}_3\text{B}\ (k_4)$$

$$\{\text{RBAX}^{\bullet-}\ n\text{-Bu}^\bullet\} \rightarrow \text{bleaching product}\ (k_5)$$

$$\{\text{RBAX}^{\bullet-}\ n\text{-Bu}^\bullet\} \rightarrow \text{RBAX}^{\bullet-} + n\text{-Bu}^\bullet\ (k_6)$$

$$\text{RBAX}^{\bullet-} \rightarrow \text{RB} + \text{Ac}^\bullet\ (k_7)$$

From laser flash photolysis measurements we obtain $k_1 = 2.78 \times 10^5\ \text{s}^{-1}$ and $k_1 + k_2[\text{O}_2] = 3.47 \times 10^6\ \text{s}^{-1}$ in air. The quantum yields are given by

$$\phi(-\text{RBAX}) = \phi_T k_4[\text{Bo}^-]/(k_1 + k_2[\text{O}_2] + (k_3 + k_4)[\text{Bo}^-])$$

$$\phi(\text{RB}) = (k_5/k_5 + k_6)\phi(-\text{RBAX})$$

The observation that the rate of RB generation varies linearly with the absorbed light intensity is evidence that the radicals $\text{RBAX}^{\bullet-}$ and *n*-$\text{Bu}^\bullet$ do not undergo significant recombination after dissociation of the geminate pair. Similarly, the independence of $\phi(\text{RB})/\phi(-\text{RBAX})$ on the presence of air indicates that $\text{RBAX}^{\bullet-}$ is not significantly quenched by oxygen during the lifetime of the radical. Evidence for the lack of oxygen quenching of the geminate pair is presented below. Assuming that oxidation of $\text{RBAX}^{\bullet-}$ by oxygen is diffusion-controlled, we obtain a minimum value for k_7 of $4 \times 10^8\ \text{s}^{-1}$.

The ratio $\phi(\text{RB})/\phi(-\text{RBAX})$ is equal to $(8.6 \pm 1.2) \times 10^{-2}$. From this value we derive $k_5/k_6 = 10.6 \pm 1.6$. Referring to Figure 7, we identify

$$A = \phi_T k_4/(k_3 + k_4) = 0.39 \pm 0.03$$

$$B = (k_1 + k_2[\text{O}_2])/(k_3 + k_4) = (4.16 \pm 0.21) \times 10^{-3}\ \text{M}$$

By introducing the lifetime of RBAX triplet in the presence of air, we derive $k_3 + k_4 = (8.35 \pm 0.42) \times 10^8\ \text{M}^{-1}\ \text{s}^{-1}$. Table I presents a summary of the different parameters we have derived from the mechanism along with the rate constants measured by laser flash photolysis.

Table I
Parameters Derived for the Mechanism Presented in Scheme I (Unless Otherwise Specified, Uncertainty ±5%)

parameter	value
k_1	$2.78 \times 10^5\ \text{s}^{-1}$
$k_1 + k_2[\text{O}_2]$	$3.47 \times 10^6\ \text{s}^{-1}$
$k_3 + k_4$	$8.35 \times 10^8\ \text{M}^{-1}\ \text{s}^{-1}$
k_7	$>4 \times 10^8\ \text{s}^{-1}$
k_5/k_6	10.6 ● 1.6
$\phi_T k_4/(k_3 + k_4)$	0.39 ± 0.03

Table II
Photoreduction Quantum Yields for Derivatives in Figure 3 in Aerated Ethyl Acetate (Dye and Borate Ion Concentrations 0.15 and 2.1 mM, Respectively)

deriv	φ(-dye)	φ(RB)	φ(RB)/φ(-dye)
1	0.132	1.07×10^{-2}	8.1×10^{-2}
2	0.115	9.31×10^{-3}	8.1×10^{-2}
3	0.135	9.56×10^{-3}	7.1×10^{-2}
4	0.153	1.38×10^{-2}	9.0×10^{-2}
5	0.113	9.69×10^{-3}	8.6×10^{-2}
6	0.129	1.08×10^{-2}	8.4×10^{-2}

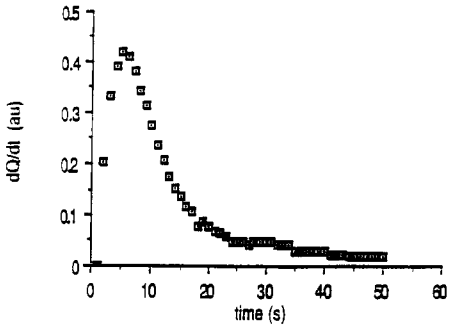

Figure 8. Rate of heat evolution during the photopolymerization of 85% TMPTA/15% HDDA: [RBAX] = 5.0×10^{-4} M, $[\text{Bo}^-] = 1.0 \times 10^{-2}$ M, $I_a = 1.7 \times 10^{-3}$ einsteins/L s.

In argon-saturated solution and for $[\text{Bo}^-] = 1.89 \times 10^{-3}$ M, the quantum yield for consumption of RBAX is 0.31. From this value we calculate $\phi_T k_4/(k_3 + k_4) = 0.37$ in argon-saturated solution and conclude that the geminate pair (see Scheme I) does not react with oxygen, as deactivation of the geminate pair will affect the photoreduction quantum yield at infinite borate concentration.

Table II presents the quantum yields of photoreduction and RB generation in aerated ethyl acetate for the six derivatives shown in Figure 3. The ratio $\phi(\text{RB})/\phi_{(-\text{dye})}$ is independent of the identity of the radical generated by cleavage of the semireduced dye (reaction with k_7 in Scheme I). The free energy of formation of these radicals in the gas phase[16] range from 3.1 kcal/mol for $\phi(\text{C=O}^\bullet)$ to −67 kcal/mol (calculated) for $(\text{Me})_2\text{CHOC=O}^\bullet$. We would expect the ratio $\phi(\text{RB})/\phi_{(-\text{dye})}$ to depend on the nature of the radical released if cleavage of the semireduced dye occurred in the geminate pair since it would compete with the formation of bleaching product. However, as we show in the section on photopolymerization in thick samples, the nature of this radical has only a moderate though significant effect on the rate of photopolymerization.

Photopolymerization in Thin Films. Figure 8 shows the rate of heat evolution (in arbitrary units) during a photopolymerization experiment. The area under the curve is proportional to the number of double bonds reacted. Determination of the area for experiments performed with different light intensities and Bo^- con-

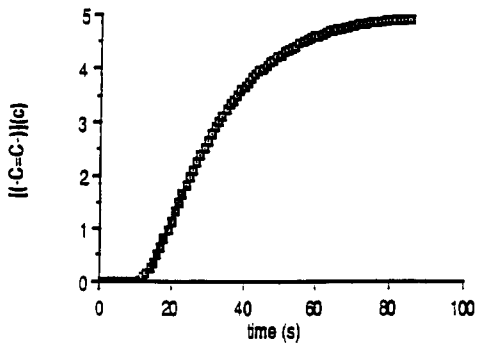

Figure 9. Concentration of double bonds reacted against irradiation time: 85% TMPTA/15% HDDA, [RBAX] = 5.0×10^{-4} M, [Bo$^-$] = 1.0×10^{-2} M, $I_a = 1.06 \times 10^{-4}$ einsteins/L s.

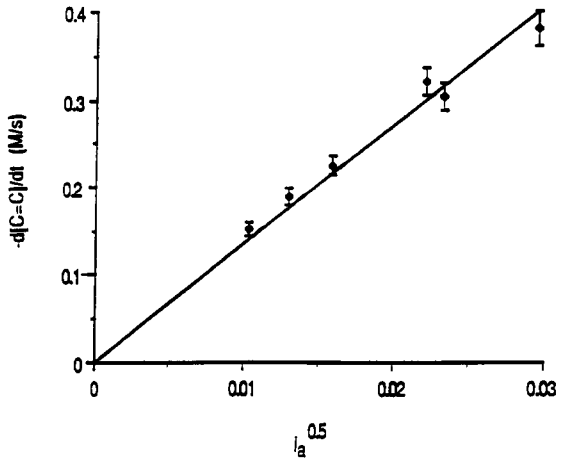

Figure 10. Effect of light intensity on the initial rate of photopolymerization: 85% TMPTA/15% HDDA, [RBAX] = 5.0×10^{-4} M, [Bo$^-$] = 1.0×10^{-2} M. The slope of the line is 13.5 ± 0.3 (M/s) (einsteins/L s)$^{-0.5}$.

centrations indicates that the number of double bonds consumed is independent of the absorbed intensity and Bo$^-$ concentration. Measurement of the absorbance at 810 cm^{-1} before irradiation and after cessation of the reaction yields a value for the maximum conversion of 45%, or 4.86 M.

Using the value for the maximum conversion obtained above, we construct a plot of concentration of double bonds consumed as a function of irradiation time (Figure 9). From the initial slope we obtain the rate of photopolymerization at low conversion and the intercept with the time axis gives a value for the induction period which is clearly observable at this low light intensity (16 times lower than that shown in Figure 8).

The induction period obtained from Figure 9 is 12.8 s. At a constant Bo$^-$ concentration of 10 mM the reciprocal of the induction period increases linearly with the absorbed intensity ($I_a = (1\text{–}8) \times 10^{-4}$ einsteins/L s), the slope of the line being 404 ± 65 L/einsteins. For an absorbed intensity of 6.86×10^{-4} einsteins/L s we obtain that the induction period is independent of the Bo$^-$ concentration. The average value is 3.4 ± 0.6 s for [Bo$^-$] = 0.8–20 mM.

The initial rate of photopolymerization calculated from Figure 9 is 0.151 M/s. The order with respect to light intensity is 0.5 (Figure 10), and at constant intensity the rate of photopolymerization is independent of the Bo$^-$ concentration (Figure 11). On the basis of these results we write for the initial rate of photopolymerization

$$R_p = [M]_0 R_i^{0.5} k_p / k_t^{0.5}$$

where $[M]_0$ is the initial concentration of double bonds (10.8 M), R_i the rate of initiation, and k_p and k_t the rate

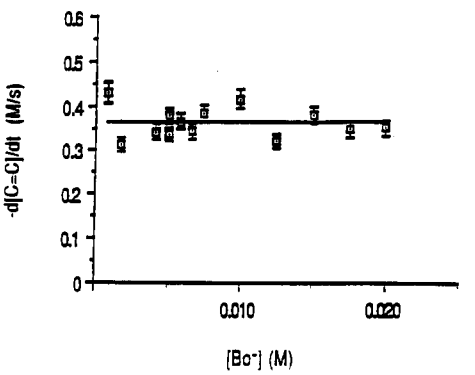

Figure 11. Plot of the initial rate of photopolymerization against the concentration of triphenyl *n*-butyl borate ion: [RBAX] = 5.0×10^{-4} M, $I_a = 6.84 \times 10^{-4}$ einstein/L s. The average value for the rate of photopolymerization is 0.36 ± 0.03 M/s.

Table III
Parameters Derived for the Photopolymerization of 15% HDDA/85% TMPTA with RBAX (0.5 mM) and Triphenyl *n*-Butyl Borate Ion at 514 nm (Absorbed Light Intensity (I_a) in einsteins/L s)

parameter	value
R_p	$(13.5 \pm 0.3) I_a^{0.5}$
ϕ_p	1420[a]
ϕ_i	0.067 ± 0.009
kcl[b]	$(2.1 \pm 0.3) \times 10^4$
$k_p/k_t^{0.5}$	4.8 ± 0.4 M$^{-0.5}$ s$^{-0.5}$

[a] $I_a = 1.06 \times 10^{-4}$. [b] Kinetic chain length. $I_a = 1.06 \times 10^{-4}$.

constants for propagation and bimolecular termination, respectively. The rate of initiation, equal to twice the rate of RB generation, is given by (see Scheme I)

$$R_i = \alpha I_a \phi_T k_4 [Bo^-] / (k_1 + k_2[O_2] + (k_3 + k_4)[Bo^-])$$

with $\alpha = 0.17 \pm 0.02$.

Measurements of the lifetime of RBAX triplet in the monomer formulation yield values of 3.2 and 1.6 μs in argon-saturated samples and in the presence of air, respectively. The results shown in Figure 11 indicate that the photopolymerization order with respect to Bo$^-$ is zero, implying that $k_3 + k_4$ is greater than 3×10^9 M^{-1} s^{-1}. The rate constant calculated for a diffusion-controlled reaction[17] in this monomer formulation is 1.7×10^8 M^{-1} s^{-1}, and we conclude that under these conditions quenching of RBAX excited state occurs, at least partially, by a static mechanism not requiring diffusion.

The quantum yield of photopolymerization, as well as the kinetic chain length (ϕ_p/ϕ_i), decreases with the square root of the absorbed light intensity. For the conditions shown in Figure 9 the photopolymerization quantum yield is 1420. The quantum yield for radical generation is 0.067, giving a kinetic chain length of 2.1×10^4, which compares favorably with the value of 2.9×10^4 reported for the UV photopolymerization of epoxy diacrylate/TMPTA in the presence of air.[18] From the slope of the line in Figure 10 and introducing the appropriate values in the equation for R_p, we obtain $k_p/k_t^{0.5} = 4.8 \pm 0.4$ M$^{-0.5}$ s$^{-0.5}$. A summary of these parameters is presented in Table III. The value of $k_p/k_t^{0.5}$ for diallyloxydiethylene dicarbonate is 1.5 ± 0.2[19] whereas that obtained for dimethacrylates[20] ranges from 0.7 to 2.2 M$^{-0.5}$ s$^{-0.5}$. The higher value obtained for our system is indicative of faster propagation, slower termination, or both.

Photopolymerization of the system we have studied appears to proceed by the conventional mechanism in which termination occurs by reaction between two macroradicals. The same mechanism has been found to be valid for the UV photopolymerization of diallyloxydieth-

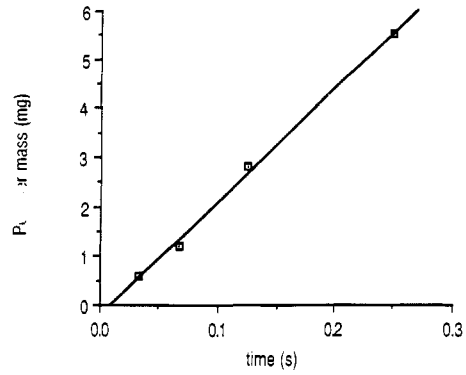

Figure 12. Mass of solid spike produced against irradiation time: 90% DPHPA/10% VP, [RBAX] = 0.5 mM, [NPG] = 50 mM, laser power density 7.3 W/cm^2. The slope of the line is 22.9 mg/s.

ylene dicarbonate at low conversions,[18] polyurethane–diacrylate/diacrylate diluent systems studied by Decker and Moussa,[21] and for the visible photopolymerization (at low conversions) of TMPTA in microcapsules.[22]

Previous work by Decker[23] and Decker and Moussa[24,25] shows a linear dependence on light intensity for the UV photopolymerization of their monomer systems, implying the participation of a unimolecular termination step. In the case of diallyloxydiethylene dicarbonate, Bellobono et al.[19] find that radical occlusion and bimolecular reaction occur simultaneously, their contribution to the overall termination depending on the conversion. Analysis of the thin foil photocalorimetry traces at different light intensities for our initiator/monomer system shows no evidence for a conversion-dependent order with respect to light intensity up to conversions approaching 40%, indicating that bimolecular termination is predominant even at relatively high conversions.

Photopolymerization in Thick Samples. In this section we describe our photopolymerization results obtained with power densities higher than 1 W/cm^2 at 514 nm and nonexpanded laser beam diameter (1.4 mm). The volume of sample irradiated is a small fraction of the total, simulating the conditions found in stereolithography.[9] Because of bleaching of the initiator, the reaction may occur at depth as well as at the surface, and irradiation generates a solid spike (Figure 4), the dimensions of which depend on the irradiation time and the laser power.

We have measured the rate of photopolymerization by isolating the formed spike and measuring its weight. To prevent losses during the isolation step, the solid must be strong and this limits the kind of formulation we can study using this methodology. An appropriate monomer formulation is 90% dipentaerythritol hydroxypentaacrylate (DPHPA) and 10% 1-vinyl-2-pyrrolidinone (VP). The experiments described below were carried out using *N*-phenylglycine (NPG) as an electron donor since we found it was twice as fast as borate at the same concentration.

Figure 12 shows a plot of polymer mass as a function of irradiation time for 0.5 mM RBAX irradiated with power density of 7.3 W/cm^2 in the presence of 50 mM NPG. The slope of the line yields a value of 22.9 mg/s for the rate of photopolymerization. Experiments performed with different power densities in the range from 3 to 12 W/cm^2 indicate that the rate of photopolymerization varies with the square root of the laser intensity.

Table IV presents the rate of photopolymerization measured for the six derivatives shown in Figure 3 and the values of $k_p/k_t^{0.5}$ (relative to RBAX)[26] derived by combining the rate of photopolymerization with the quantum yields of RB generation presented in Table II.

Table IV
Photopolymerization Rates and Relative Values of $k_p/k_t^{0.5}$ for the Compounds in Figure 3 (Monomer Formulation, 90% DPHPA/10% VP; Dye and NPG Concentrations, 0.5 and 50 mM, Respectively; Laser Power Density, 7.3 W/cm^2 (514 nm))

dye	rate (mg/s)	$k_p/k_t^{0.5}$ (rel to RBAX, dye 1)
1	22.9	1
2	26.1	1.22
3	31.1	1.43
4	23.1	0.89
5	31.0	1.42
6	29.6	1.28

Table V
Relative Rate Constants of Termination between a Polymer Radical and $R_2^\bullet$ (See Scheme II)

$R_2^\bullet$	$k_t(R_2^\bullet)/k_t(CH_3C{=}O^\bullet)$
$CH_3C{=}O^\bullet$	1.00
$PhC{=}O^\bullet$	0.67
$(MeO)_3PhC{=}O^\bullet$	0.48
$PhCH_2OC{=}O^\bullet$	1.26
$EtOC{=}O^\bullet$	0.50
$(Me)_2CHOC{=}O^\bullet$	0.61

Because the rate constant of propagation is independent of the identity of the initiating radical, the variation of $k_p/k_t^{0.5}$ shown in Table IV must be due to different rate constants for termination. Because the rate constant for termination between two macroradicals is independent of the initiating radical, we interpret these results as evidence that small initiating radicals are involved in the termination process. However, as a reviewer points out, the dependence of k_t on the identity of the initiator does not exclude a contribution of bimolecular termination between two polymer radicals. To estimate this contribution, we have synthesized an ester derivative of RB containing a polystyrene fragment of molecular weight equal to 90 000 (R = polystyrene in Figure 3). Details of the synthesis and the kinetics of photopolymerization using this initiator will be published in a separate communication.[27] Of relevance to the results presented in Table IV is the observation that with this polymeric initiator the rate of polymerization varies linearly with the laser intensity, indicating that bimolecular termination between polymer radicals is too slow to be competitive with radical occlusion. Therefore, we conclude that in our systems, for which we observe half order with respect to light intensity even at high conversions, termination occurs not by reaction between two polymer radicals but between one macroradical and one small radical, the latter being produced by cleavage of the semireduced dye initiator.

Scheme II presents a general mechanism consistent with the photopolymerization results we observe with our photoinitiators and electron donors. Table V shows relative values of termination rate constants for the radicals generated by cleavage of semireduced dye. Most of the radicals are less effective terminators than acetyl with the exception of $PhCH_2OC{=}O^\bullet$, which can easily lose carbon dioxide to generate the benzyl radical.

The radicals shown in Table V are expected to be good initiators. We would expect them to add to unreacted monomer as soon as they are produced and, as a consequence, not to be available for termination when the photopolymerization is carried out under steady-state irradiation. However, our results indicate these radicals are the main chain terminators in our systems. We postulate that this effect is partially due to $RBAX^{\bullet-}$ being a long-lived species in the monomers we have employed in this work. From our bleaching results we estimate a lifetime shorter than 3 ns for $RBAX^{\bullet-}$ in ethyl acetate (Table I). It is possible the high viscosities of TMPTA (65 cP) and

Scheme II

$$\text{dye} + \text{donor} \xrightarrow{h\nu} \text{dye}^{\bullet-} + (\text{donor})^{\bullet+} \quad (I_a\phi_i)$$

$$(\text{donor})^{\bullet+} \rightarrow R_1^{\bullet} + \text{acid}$$

$$\text{dye}^{\bullet-} \rightarrow R_2^{\bullet} + \text{RB}$$

propagation

$$R_1^{\bullet} + M \rightarrow M_1^{\bullet}$$

$$M_1^{\bullet} + M \rightarrow M_2^{\bullet}$$

$$M_{n-1}^{\bullet} + M \rightarrow M_n^{\bullet}$$

termination

$$M_n^{\bullet} + R_2^{\bullet} \rightarrow \text{inert polymer}$$

$R_2^{\bullet}$ = acetyl when dye = RBAX (see Figure 3); acid = Ph_3B when donor = triphenyl *n*-butyl borate ion; acid = H^+ when donor = *N*-phenylglycine

DPHPA (6000 cP) have a retarding effect on the cleavage of $RBAX^{\bullet-}$ so that the polymerization can propagate to a considerable extent before the terminator radical is generated.

Summary

We have prepared six ester derivatives of decarboxylated Rose Bengal which are suitable as electron-transfer photoinitiators at the wavelengths of the Ar^+ laser.

Photoreduction of the dyes (Figure 3) by triphenyl *n*-butyl borate ion (Bo^-) in ethyl acetate produces decarboxylated Rose Bengal (RB) as well as bleaching products, RB being generated by cleavage of the radical anion formed in the initial electron-transfer step. Quantum yields of dye consumption, with $[Bo^-] = 2.1 \times 10^{-3}$ M, are in the 0.11–0.15 range. $\phi(RB)/\phi_{(-dye)}$ is approximately 0.08, and for RBAX we have determined the ratio is independent of borate concentration, light intensity, and the presence of oxygen.

Photopolymerization of 85% TMPTA/15% HDDA was studied by thin foil photocalorimetry using RBAX and borate as photoinitiator. Photoreduction of the dyes in Figure 3 with *N*-phenylglycine was used to initiate the polymerization of 90% DPHPA/10% VP in thick samples. Our results indicate the rate of photopolymerization increases linearly with the square root of the light intensity bot at low and high conversions. The ratio $k_p/k_t^{0.5}$ depends on the identity of the RB ester (Figure 3) employed as photoinitiator. On the basis of our kinetics results, we propose a mechanism for the photopolymerization in which the initiating radical is derived from the electron donor whereas the radical generated by cleavage of semireduced dye acts as the predominant terminator of polymer chains.

Acknowledgment. This work has been supported in part by the Ohio Department of Development, Thomas Edison Program, in part by Ciba-Geigy (Plastics Division, Marly, Switzerland), and in part by the National Science Foundation (Grant DMR 9013109). We are most grateful for the support of these donors.

References and Notes

(1) Contribution No. 119 from the Center for Photochemical Sciences.
(2) Pappas, S. P. *Photocuring; Principles and Applications*; Scientific Enterprise: Norwalk, CT, 1978.
(3) Color It Smart. *Forbes Magazine* Oct 18, 1988.
(4) Cycolor is a trademark of Mead Corp.
(5) Linden, M.; Neckers, D. C. Onium Salts of Xanthene Dyes. U.S. Patent Application. See, for example: Neckers, D. C.; Chesneau, E. Electron Transfer Sensitized Photobleaching of Rose Bengal Induced by Triplet Benzophenones. *J. Photochem.* **1988**, *42*, 269. Linden, S. M.; Neckers, D. C. Bleaching Studies of Rose Bengal Onium Salts. *J. Am. Chem. Soc.* **1988**, *110*, 1257.
(6) The principal investigator has written extensively on the photochemistry and spectroscopy of the xanthenes. Little detail will be provided here. The interested reader is referred to some of these recent reviews. See, for example: Valdes-Aguilera, O.; Neckers, D. C. *Acc. Chem. Res.*, in press. Neckers, D. C. *J. Chem. Educ.* **1987**, *64*, 649. Neckers, D. C. *J. Photochem. Photobiol.* **1989**, *44*, 1.
(7) Zakrewski, A.; Neckers, D. C. Tetrahedron, *Tetrahedron* **1987**, *43*, 4507, and references cited therein.
(8) Neckers, D. C.; Raghuveer, K. S.; Valdes-Aguilera, O. *Polym. Materials Sci. Eng.* **1989**, *60*, 15.
(9) Stereolithography. See: Hull, C. J.S. Patent 4,575,330, March 11, 1986.
(10) See, for example: Valdes-Aguilera, O.; Neckers, D. C. *Acc. Chem. Res.*, in press. Neckers, D. C. *J. Chem. Educ.* **1987**, *64*, 649. Neckers, D. C. *J. Photochem. Photobiol.* **1989**, *44*, 1. Neckers, D. C.; Valdes-Aguilera, O. M. *Adv. Photochem.*, in press.
(11) Amat-Guerri, F.; Lopez-Gonzalez, M. M. C.; Martinez-Utrilla, R. *Tetrahedron Lett.* **1984**, *38*, 4285.
(12) Hoyle, C. E.; Kim, K.-J. *Appl. Polym. Sci.* **1987**, *33*, 2985 and references therein.
(13) Chatterjee, S.; Gottschalk, P.; Davis, P. D.; Schuster, G. B. *J. Am. Chem. Soc.* **1988**, *110*, 2326.
(14) See, for example: Lamberts, J. J. M.; Schumacher, D. R.; Neckers, D. C. *J. Am. Chem. Soc.* **1984**, *106*, 5879. Paczkowski, J.; Lamberts, J. J. M.; Paczkowska, B.; Neckers, D. C. *J. Free Radicals Biol. Med.* **1985**, *1*, 341. Xu, D.; VanLoon, A.; Linden, S. M.; Neckers, D. C. *J. Photochem.* **1987**, *38*, 357.
(15) The triplet of RBAX is monitored at 610 nm. We will report our complete flash photolysis study in a future publication.
(16) Benson, S. W. *Thermochemical Kinetics*; Wiley: New York, 1976.
(17) Murov, S. L. *Handbook of Photochemistry*; Marcel Dekker: New York, 1973.
(18) Decker, C.; Bendaikha, T. *Eur. Polym. J.* **1984**, *20*, 753.
(19) Bellobono, I. R.; Selli, E.; Righetto, L. *Makromol. Chem.* **1989**, *190*, 1945.
(20) Berlin, A. A.; Matvejeva, N. G. *J. Polym. Sci. Macromol. Rev.* **1980**, *15*, 107.
(21) Decker, C.; Moussa, K. *Makromol. Chem.* **1990**, *191*, 963.
(22) Arney, J. Private communication.
(23) Decker, C. In *Materials for Microlithography: Radiation Sensitive Polymers*; Thompson, G., Willson, G., Frechet, J., Eds.; ACS Symposium Series 266; American Chemical Society: Washington, DC, 1984; p 208.
(24) Decker, C.; Moussa, K. *Makromol. Chem.* **1988**, *189*, 2381.
(25) Decker, C.; Moussa, K. *J. Appl. Polym. Sci.* **1987**, *34*, 1603 and references therein.
(26) As is true for RBAX, the order with respect to light intensity for derivative 3 (Figure 3) is 0.5 and we can assume the same is valid for the other four compounds.
(27) Paczkowski, J.; Paczkowska, B.; Neckers, D. C. To be submitted.

Registry No. I (R = Me), 133433-82-6; I (R = C_6H_5), 137769-03-0; I (R = $C_6H_2(OMe)_3$), 137769-04-1; I (R = $OCH_2C_6H_5$), 137769-05-2; I (R = OEt), 137769-06-3; I (R = $OCH(Me)_2$), 137769-07-4; HDDA, 13048-33-4; TMPTA, 15625-89-5; HDDA/TMPTA (copolymer), 74309-76-5; DPHPA, 60506-81-2; VP, 88-12-0; DPHPA/VP (copolymer), 105759-55-5; Bo^-, 47252-39-1.